PROBLEMY MECHATRONIKI
UZBROJENIE, LOTNICTWO, INŻYNIERIA BEZPIECZEŃSTWA

ISSN 2081-5891

8, 3 (29), 2017, 73-86

PROBLEMS OF MECHATRONICS
ARMAMENT, AVIATION, SAFETY ENGINEERING

Determination of Dynamic Reactions in the Rotor Bearings of a New Design of a Seeker Head

Daniel GAPIŃSKI

Kielce University of Technology, Faculty of Mechatronics and Mechanical Engineering,
7 1000-lecia PP Avenue, 25-314 Kielce, Poland
author's e-mail address: tu_daniel_kielce@wp.pl

Received by the editorial staff on 13 June 2016.
The reviewed and verified version was received on 1 January 2017.

DOI 10.5604/01.3001.0010.4111

Abstract. This paper discusses tests designed to determine the dynamic reactions occurring in the bearings installed as aligned with the axis of rotation of a rotor for a new design of IR seeker. The seeker is intended to detect and track airborne targets that emit electromagnetic radiation in the infrared spectrum. The tests included dynamic reactions from the rotation of the rotor and reactions from the overloads applied to the seeker during the flight of its rocket missile. The test results are represented in a graphic format.
Keywords: dynamic reactions, mechatronics, homing missile seeker, target detection and tracking

1. INTRODUCTION

IR homing seekers require a very high precision of manufacturing [1, 2]. The design solutions for these products are constantly improved [3, 4, 5],

This work has been compiled from the paper presented during the 11th International Armament Conference on Scientific Aspects of Armament and Safety Technology, Ryn, Poland, September 19-22, 2016.

since the detection and position determination of a target in actual combat conditions requires ever-increasing operating precision and speed [6]. The rocket missiles equipped with IR homing seekers must also meet increasingly stringent requirements. IR homing missiles have seen improvements in both manoeuvrability and flight speed; both increase the overloading forces applied to the homing seekers. The seeker rotor is a critical component that is most exposed to dynamic overload. It is therefore important to determine the overload values present in the rotor mounting.

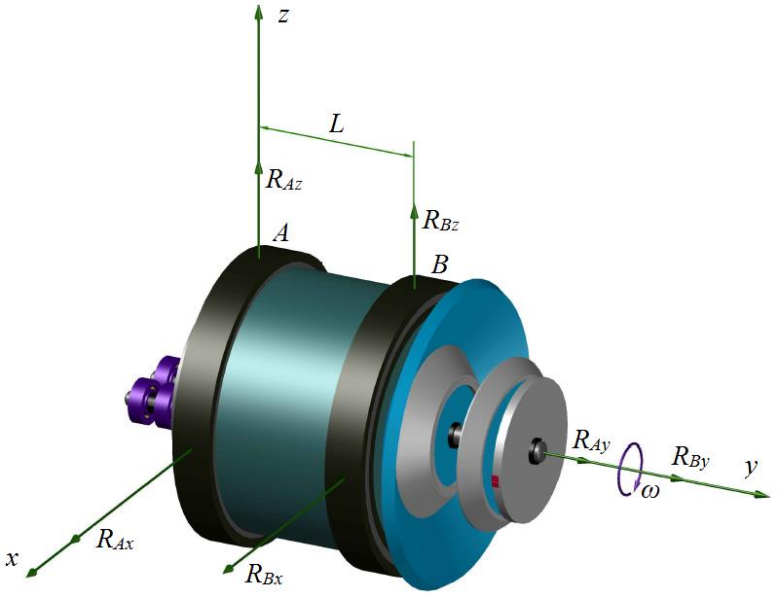

Fig. 1. Seeker rotor

Figure 1 presents a 3D model of the rotor for the designed optoelectronic seeker [7]. The seeker's design and operating principles are explained in [8]. To effectively track manoeuvring airborne targets operating at supersonic speeds, the rotor rotational speed optimal for the operating specifications of the seeker was established at 10000 rpm [9]. During the seeker's pre-programmed search in the air space and tracking of a detected target, unfavourable inputs may occur from the dynamic reactions of the seeker's rotor bearings. The largest contributor to these dynamic reactions will be the dynamic imbalance of the rotor and the longitudinal overloads from the launch of the rocket missile, as well as the lateral overloads from the rocket missile's manoeuvres along the flight trajectory. Both contributors are construed as interferences in the proper determination of the angular coordinates of the air target detected by the seeker. Determining the values of these dynamic loads sets the preconditions for the optimum selection of the bearings for the seeker rotor.

2. MATHEMATICAL MODEL

Figure 1 shows the rotor of the new seeker design. Once ramped up to its operating speed, the rotor revolves at a constant angular velocity ω along its axis of rotation that is supported by bearing A and bearing B. If the rotor angular velocity is kept steady, the total of the moments relative to the axis of rotation is zero for all external forces applied to the spinning rotor. Hence, it is appropriate to focus on determining additional reactions within bearing A and bearing B from the rotor's rotational motion and the longitudinal and lateral overloads from the movement of the rocket missile, or the dynamic reactions of the rotor. A stationary coordinate system *x*, *y*, *z* for this determination analysis with axis y aligned with the rotor's axis of rotation.

The rotor's dynamic reactions R_A and R_B to be determined were split into the components R_{Ax}, R_{Ay}, R_{Az} and R_{Bx}, R_{By}, R_{Bz}, as shown in Fig. 2.

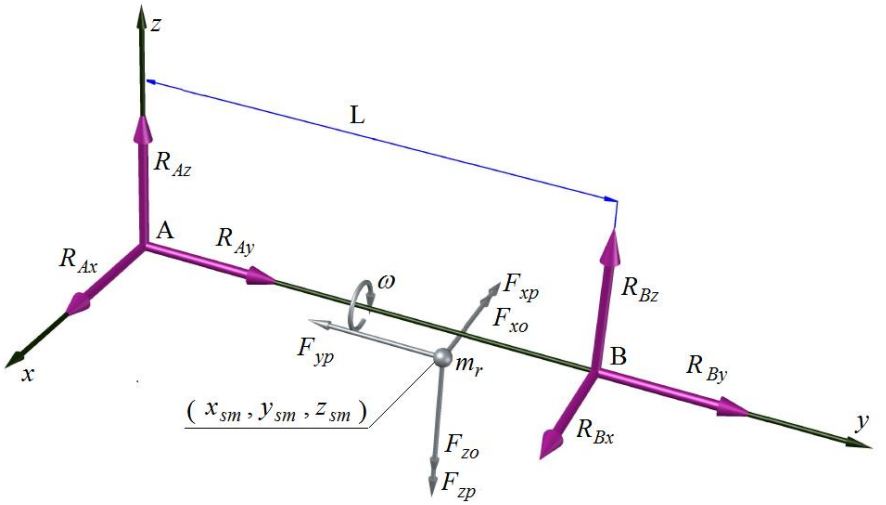

Fig. 2. Forces applied to the seeker's rotor

These components can be determined with d'Alembert's principle, by which dynamic reactions are compensated for by the forces of inertia. If the total rotor weight is m_r and it is focused in a material point designated as such and described with the coordinates x_{sm}, y_{sm}, z_{sm}, which define the rotor's centre of mass position relative to the stationary coordinate system *x*, *y*, *z*, then, given the fixed rotational speed ω, the force of inertia of this material point is a component of the centrifugal force $\vec{F}_o = \vec{\omega}^2 r\, m_r$ and of the overload force $\vec{F}_p = \vec{a}_p\, m_r$, where *r* is the distance of the point m_r to the rotation axis *y*, whereas a_p is the acceleration of the rocket missile of the seeker. The centrifugal force perpendicular to the rotation axis *y* can be split into two components parallel to the *x* and *z* axis.

These components are $F_{xo} = F_o \cdot \cos(\omega \cdot t)$ and $F_{zo} = F_o \cdot \sin(\omega \cdot t)$. The overload force can be split into three components parallel to the *x*, *y* and *z* axis. These components are, respectively: $F_{xp} = a_x\, m_r$, $F_{yp} = a_y\, m_r$ and $F_{zp} = a_z\, m_r$, where a_x, a_y and a_z are projections of the vector $\vec{a}$ on the following axes, which are respectively: *x*, *y*, *z* of the stationary coordinate system.

The total reactions within the seeker rotor bearings are described by the following relations:

$$\begin{aligned} R_{Ax} &= F_{xo} + F_{xp} - \frac{1}{L} \cdot (F_{xo} \cdot y_{sm} + F_{xp} \cdot y_{sm} - F_{yp} \cdot x_{sm}) = \\ &= \omega^2 \cdot r \cdot m_r \cdot \cos(\omega \cdot t) + a_x \cdot m_r - \frac{1}{L} \cdot (\omega^2 \cdot r \cdot m_r \cdot \cos(\omega \cdot t) \cdot y_{sm} + \\ &+ a_x \cdot m_r \cdot y_{sm} - a_y \cdot m_r \cdot x_{sm}) \end{aligned} \tag{1}$$

$$\begin{aligned} R_{Bx} &= \frac{1}{L} \cdot (F_{xo} \cdot y_{sm} + F_{xp} \cdot y_{sm} - F_{yp} \cdot x_{sm}) = \\ &= \frac{1}{L} \cdot (\omega^2 \cdot r \cdot m_r \cdot \cos(\omega \cdot t) \cdot y_{sm} + a_x \cdot m_r \cdot y_{sm} - a_y \cdot m_r \cdot x_{sm}) \end{aligned} \tag{2}$$

$$R_{Ay} = R_{By} = \frac{1}{2} \cdot F_{yp} = \frac{a_y \cdot m_r}{2} \tag{3}$$

$$\begin{aligned} R_{Az} &= F_{zo} + F_{zp} - \frac{1}{L} \cdot (F_{zo} \cdot y_{sm} + F_{zp} \cdot y_{sm} - F_{yp} \cdot z_{sm}) = \\ &= \omega^2 \cdot r \cdot m_r \cdot \sin(\omega \cdot t) + a_z \cdot m_r - \\ &+ \frac{1}{L} \cdot (\omega^2 \cdot r \cdot m_r \cdot \sin(\omega \cdot t) \cdot y_{sm} + a_z \cdot m_r \cdot y_{sm} - a_y \cdot m_r \cdot z_{sm}) \end{aligned} \tag{4}$$

$$\begin{aligned} R_{Bz} &= \frac{1}{L} (F_{zo} \cdot y_{sm} + F_{zp} \cdot y_{sm} - F_{yp} \cdot z_{sm}) = \\ &= \frac{1}{L} \cdot (\omega^2 \cdot r \cdot m_r \cdot \sin(\omega \cdot t) \cdot y_{sm} + \\ &+ a_z \cdot m_r \cdot y_{sm} - a_y \cdot m_r \cdot z_{sm}) \end{aligned} \tag{5}$$

To determine the approximate values of the accelerations F_{xp}, F_{yp}, and F_{zp} applied to the seeker in flight, a general kinematics model of the seeker must be formulated.

Figure 3 shows the targeting coordinate system, $x_{Cel}y_{Cel}z_{Cel}$, typical of homing rocket missiles. This targeting coordinate system with the vector $\vec{r}$ that binds the rocket missile to its target enables the determination of the position of the rocket missile relative to its target. The axis y_{Cel} is directed from the rocket missile's centre of mass P to the target's centre of mass C. The coordinate system $x_Cy_Cz_C$ is bound to the target, whereas the axis y_C is aligned with the velocity vector of the target. The coordinate system $x_py_pz_p$ is bound to the rocket missile, whereas the axis y_p is aligned with the velocity vector of the rocket missile. The coordinate system $x_Wy_Wz_W$ is the stationary coordinate system bound to the rocket missile launcher and thus an inertial frame of reference.

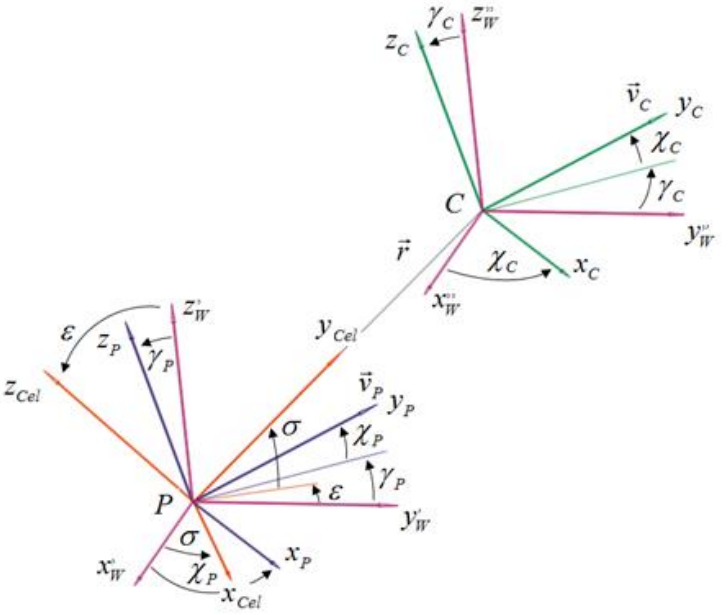

Fig. 3. Adopted coordinate systems

Based on the adopted coordinate system, kinematic relations between the rocket missile and its target were derived [10]:

$$\frac{dr}{dt} = v_C \cdot \left[\cos(\chi_C)\cdot\cos(\sigma)\cdot\cos(\varepsilon-\gamma_C)+\sin(\chi_C)\cdot\sin(\sigma)\right]+ \\ -v_P \cdot \left[\cos(\chi_P)\cdot\cos(\sigma)\cdot\cos(\varepsilon-\gamma_P)+\sin(\chi_P)\cdot\sin(\sigma)\right] \tag{6}$$

$$\frac{d\varepsilon}{dt} = \frac{-v_C\cdot\cos(\chi_C)\cdot\sin(\varepsilon-\gamma_C)+v_P\cdot\cos(\chi_P)\cdot\sin(\varepsilon-\gamma_P)}{r\cdot\cos(\sigma)} \tag{7}$$

$$\frac{d\sigma}{dt} = \{ -v_C \cdot [\cos(\chi_C) \cdot \sin(\sigma) \cdot \cos(\varepsilon - \gamma_C) - \sin(\chi_C) \cdot \cos(\sigma)] + \\ + v_P [\cos(\chi_P) \cdot \sin(\sigma) \cdot \cos(\varepsilon - \gamma_P) - \sin(\chi_P) \cdot \cos(\sigma)] \} / r \tag{8}$$

where:

v_C – target velocity,
v_P – rocket missile velocity,
γ_P, χ_P – rocket missile flight angles,
γ_C, χ_C – target flight angles,
ε, σ – target observation angles,
r – distance from the rocket missile to the target.

Through equations (6) to (8), the method of homing the rocket missile in on the target can be expressed by what is referred to as the proportional navigation method [11, 12]:

$$\frac{d\gamma_p}{dt} = a_1 \frac{d\varepsilon}{dt} \tag{9}$$

$$\frac{d\chi_p}{dt} = a_2 \frac{d\sigma}{dt} \tag{10}$$

where:

a_1, a_2 are constant factors of the proportional navigation homing method.

Next, the overload forces applied to the rocket missile were expressed in the following kinematic form [10]:

$$n_x = \frac{v_P}{g} \cdot \dot{\chi}_P - \sin(\gamma_P) \cdot \sin(\chi_P) \tag{11}$$

$$n_y = -\frac{\dot{v}_P}{g} + \sin(\gamma_P) \cdot \cos(\chi_P) \tag{12}$$

$$n_z = -\frac{v_P}{g} \cdot \dot{\gamma}_P \cdot \cos(\chi_P) - \cos(\gamma_P) \tag{13}$$

where g is the Earth's gravitational acceleration.

The formulas (10) to (13) served to determine the approximate values of the forces F_{xp}, F_{yp} and F_{zp} applied to the seeker mid-flight of the rocket missile:

$$F_{xp} = a_x \cdot m_r = n_x \cdot g \cdot m_r \tag{14}$$

$$F_{yp} = a_y \cdot m_r = n_y \cdot g \cdot m_r \tag{15}$$

$$F_{zp} = a_z \cdot m_r = n_z \cdot g \cdot m_r \tag{16}$$

3. TEST RESULTS

The following shows a selection of the computer simulations of the dynamic loads applied to the rotor bearings of the new optoelectronic seeker design, and the resulting dynamic reactions within the seeker's rotor bearings.

3.1. Seeker rotor parameters

Rotor centre of mass relative to the axis *x*, *y*, *z*:

$$x_{sm} = 0.000234 \text{ m} ; y_{sm} = 0.028 \text{ m} ; z_{sm} = 0 \text{ m}$$

Distance of the centre of mass from the rotation axis *y*:

$$r = \sqrt{x_{sm}^2 + z_{sm}^2} = 0.000234\text{m}$$

Rotor mass: *c*.
Rotor rotational speed: $n = 1050$ rad/s ≈ 10 000 rpm
Bearing to bearing distance: $L = 0.042$ m

3.2. Determination of the dynamic reactions within the seeker rotor bearings while the rocket missile is homing in on an intercept course and without any dynamic balancing of the rotor

This simulation was completed at the target flight velocity v_c = 300 m/s. The target's position relative to the rocket missile launcher at the time of target detection by the seeker was: x_W = 50 m, y_W = 2600 m, z_W = 500 m. The distance to the target at the time of target detection by the seeker was: r = 2681 m. The distance to the target during the launch of the rocket missile was: r = 17 458 m. Fig. 4 shows the trajectories of the target and the rocket missile. (1) is the target flight trajectory over the total time delay T that determined the time from target detection to the launch of the rocket missile [13]. (2) is the target flight trajectory after the launch of the rocket missile. (3) is the rocket missile flight trajectory.

Figure 5 shows the velocity of the rocket missile. (1) is the rocket missile velocity during the launch motor burn. (2) is the rocket missile velocity during the sustainer motor burn. Figs. 6 and 7 show the overload forces applied to the rocket missile mid-flight through which the dynamic forces applied to the seeker rotor were calculated in (14) to (16). Moreover, the simulations accounted for a rotor imbalance applied as a run-out of the centre of mass imposed by the design of the device and its manufacturing inaccuracy.

Figures 12 and 13 show the total (resultant) dynamic reactions applied to the bearings of the seeker rotor mid-flight of the rocket missile. The components of the reactions listed are shown in Figs. 8 to 11 and in Fig. 18.

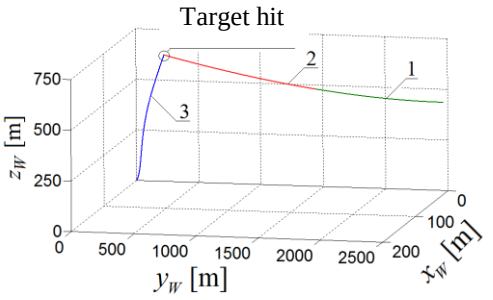

Fig. 4. Flight paths of the target and the rocket missile

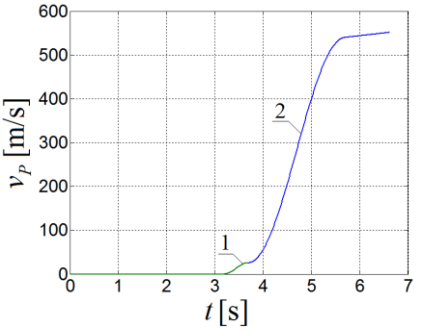

Fig. 5. Rocket missile velocity

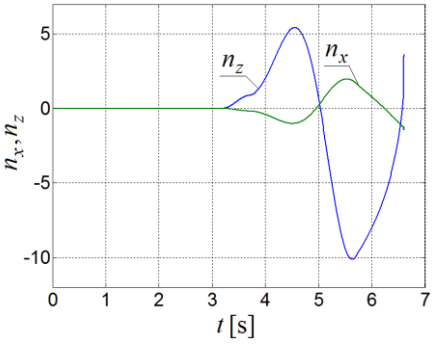

Fig. 6. Lateral overloads of the rocket missile

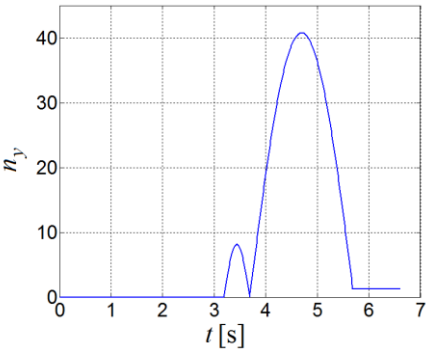

Fig. 7. Longitudinal overloads of the rocket missile

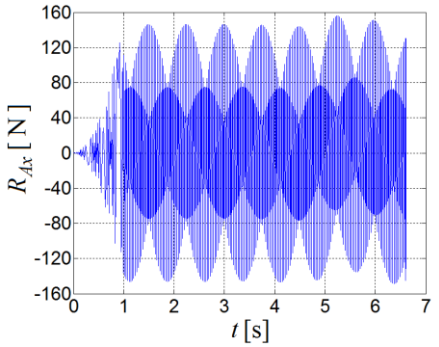

Fig. 8. Reaction R_{Ax}

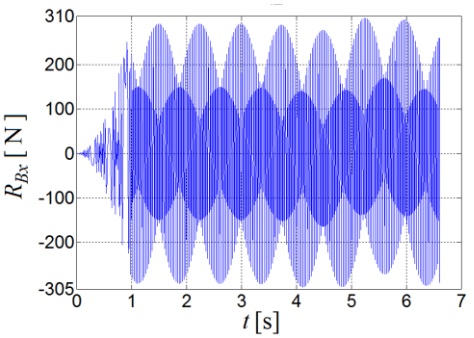

Fig. 9. Reaction R_{Bx}

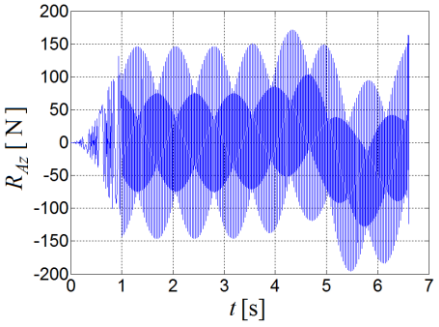

Fig. 10. Reaction R_{Az}

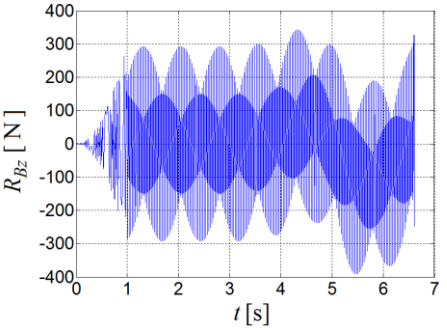

Fig. 11. Reaction R_{Bz}

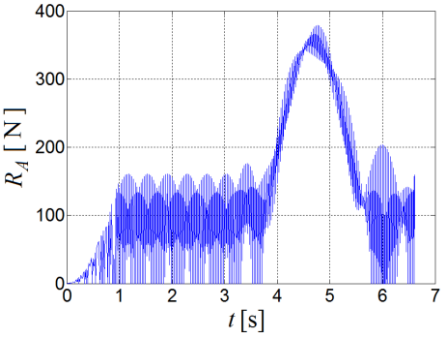

Fig. 12. Reaction R_A

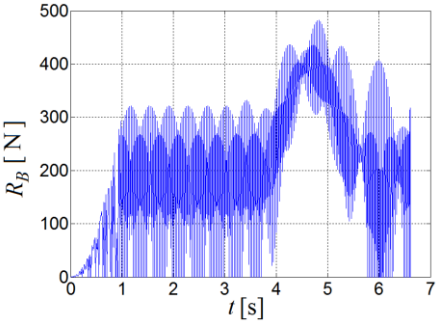

Fig. 13. Reaction R_B

3.3. Determination of the dynamic reactions within the seeker rotor bearings while the rocket missile is homing in on a trajectory shown in Section 3.2, following dynamic balancing of the rotor

The balancing of the seeker rotor should provide the best possible alignment of the rotor centre of mass m_r with the rotor rotational axis so that r is as close to zero as possible. In actual conditions, a perfect dynamic balance is not possible; however, the most perfect dynamic balance possible may reduce the dynamic reactions within the rotor bearings. In this section of the paper a dynamic balance of the rotor was adopted at one order of magnitude; hence, it was assumed that the distance of the rotor centre of mass to the rotor rotational axis was reduced to r = 0.0234 mm. The corresponding simulation results are shown in Figs. 14 to 21.

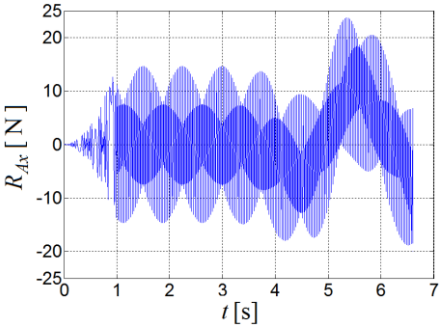

Fig. 14. Reaction R_{Ax} with dynamic balance

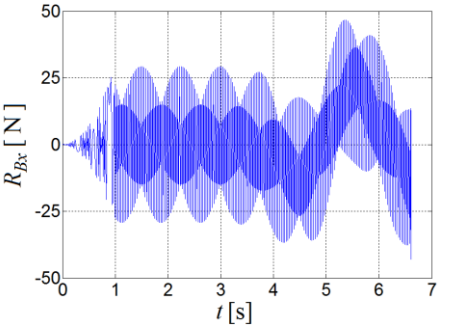

Fig. 15. Reaction R_{Bx} with dynamic balance

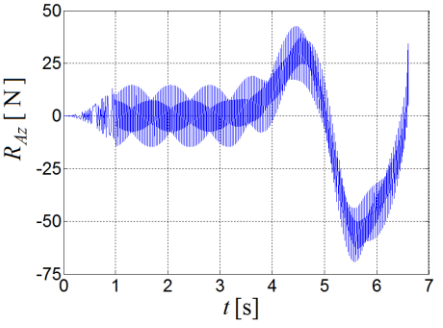

Fig. 16. Reaction R_{Az} with dynamic balance

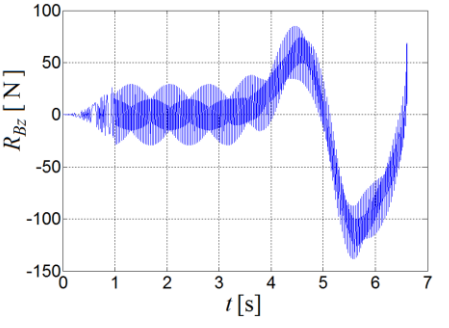

Fig. 17. Reaction R_{Bz} with dynamic balance

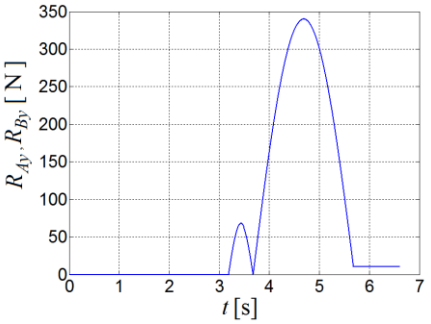

Fig. 18. Reactions R_{Ay} and R_{By}

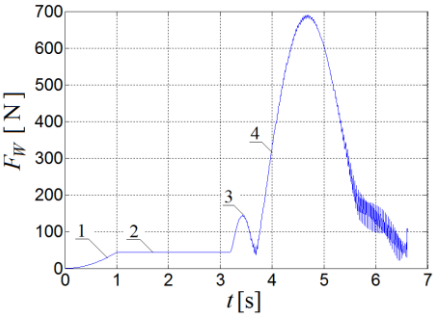

Fig. 19. Total force F_W

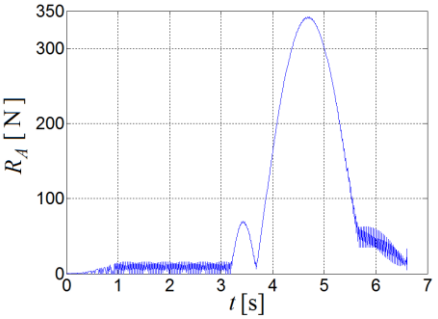

Fig. 20. Total reaction R_A with dynamic balance

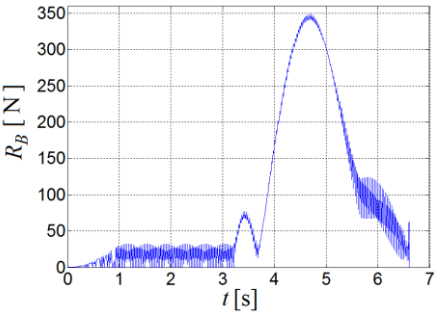

Fig. 21. Total reaction R_B with dynamic balance

Figs. 20 and 21 show the total (resultant) dynamic reactions applied to the bearings of the seeker rotor with dynamic balance. The components of the reactions listed are shown in Figs. 14 to 18. Fig. 19 shows the total (resultant) force applied to the seeker rotor. (1) is the total force applied to the rotor upon ramping its rotations. (2) is the total force applied to the rotor at the operating rotational speed. (3) is the total force applied to the rotor during the launch motor burn of the rocket missile. (4) is the total force applied to the rotor during the sustainer motor burn of the rocket missile.

4. CONCLUSION

As suggested by the completed analysis, when the seeker searches the airspace for a target and when the seeker's rocket missile is in flight, unfavourable inputs are applied to the homing seeker's rotor in the form of dynamic reactions within the rotor's bearing system.

The largest contributor to these dynamic reactions will be the dynamic imbalance of the rotor and the longitudinal overloads from the launch of the rocket missile, as well as the lateral overloads from the rocket missile's manoeuvres along the flight trajectory.

While the impact of the dynamic loads on the seeker's rotor generated during the flight of the rocket missile could not be minimized, the loads generated by the centrifugal force from the high rotational speed of the rotor can be effectively reduced by the precise balancing of the rotor. A comparison between the result sets in Section 3.2 and Section 3.3 shows that dynamic balancing produced a pronounced reduction in the lateral reaction values of the rotor bearings. A conclusion which may be drawn from these results is that with the seeker rotor balanced, the highest dynamic reaction values will occur along the lengthwise axis of the rotor. This suggests that bearings capable of sustaining axial loads should be used. When comparing the pre-balancing lateral reaction values to the post-balancing ones, it is evident that the balancing applied in this case reduced the values by a mean of ca. 467%. Balancing the rotor had no effect on the longitudinal loads applied to the bearings, however, there was an effect consisting of a reduction in the total reaction values by ca. 126%. Despite a satisfactory reduction in the dynamic axial reactions within the rotor bearings, further investigation requires a feasibility analysis for the application of additional lateral vibration dampening of the bearings, the damping frequency of which will be in tune with the angular frequency of the rotor spin that was ca. 166.7 Hz.

REFERENCES

[1] Koruba Zbigniew. 2008. *Elementy teorii i zastosowań giroskopu sterowanego.* Monografie, Studia, Rozprawy M 7. Kielce: Wydawnictwo Politechniki Świętokrzyskiej.

[2] Koruba Zbigniew. 2001. *Dynamika i sterowanie giroskopem na pokładzie obiektu latającego.* Monografie, Studia, Rozprawy 25. Kielce: Wydawnictwo Politechniki Świętokrzyskiej.

[3] RAYTHEON COMPANY. 2010. „Optical system for aide field of view staring infrared sensor having improved optical symmetry". *European Patent,* EP 1618358 B1.

[4] LFK-Lenkflugkoerpersystem GmbH. 2012. „Infrared Seeker Head". *United States Patent,* US 2012/0248238 A1.

[5] Diehl BGT Defence GmbH & Co. 2012. „Verfahren zum Steuern eines Lenkflugkörpers und Such kopf fur einen Lenkflugkörper". *Deutsches. Patent – und Markenamt,* DE 102010055493 A1.

[6] Adamski Mirosław Jan. 2009. Obrona samolotów i śmigłowców przed atakiem z ziemi i powietrza. W *Systemy przeciwlotnicze i obrony powietrznej*. Ośrodek Badawczo - Rozwojowy Sprzętu Mechanicznego Tarnów.

[7] Gapiński Daniel. 2008. „Optyczny Koordynator Skanującego dla pocisku samonaprowadzającego się na cel". *Urząd Patentowy Rzeczypospolitej Polskiej*, PL 199721 B1.

[8] Gapiński Daniel, Zbigniew Koruba, Izabela Krzysztofik. 2014. „The model of dynamics and control of modified optical scanning seeker in anti-aircraft rocket missile". *Mechanical System and Signal Processing* 45(2) : 433-447.

[9] Gapiński Daniel, Izabela Krzysztofik, Zbigniew Koruba. 2015. „Stabilność zaprojektowanego koordynatora skanującego w przeciwlotniczym pocisku rakietowym". *Problemy mechatroniki. Uzbrojenie, lotnictwo, inżynieria bezpieczeństwa – Problems of Mechatronics. Armament, Aviation, Safety Engineering* 6(1) : 56-70.

[10] Koruba Zbigniew, Jan Wojciech Osiecki. 1999. *Budowa, dynamika i nawigacja pocisków rakietowych bliskiego zasięgu.* Kielce: Skrypt Politechniki Świętokrzyskiej nr 348.

[11] Baranowski Leszek, Bogdan Machowski. 2011. „Analiza efektywności metody proporcjonalnej nawigacji w sterowaniu gazodynamicznym wirujących obiektów latających". *Problemy mechatroniki. Uzbrojenie, lotnictwo, inżynieria bezpieczeństwa – Problems of Mechatronics. Armament, Aviation, Safety Engineering* 4(1) : 37-54.

[12] Stefański Konrad, Marta Grzyb. 2013. „Porównanie efektywności metod samonaprowadzania przeciwlotniczego pocisku rakietowego sterowanego wirnikowym układem wykonawczym". *Problemy mechatroniki. Uzbrojenie, lotnictwo, inżynieria bezpieczeństwa – Problems of Mechatronics. Armament, Aviation, Safety Engineering* 4(4) : 27-39.

[13] Sztab Generalny Wojska Polskiego – Inspektorat Logistyki. 1996. *Przenośny Przeciwlotniczy Zestaw Rakietowy Grom-I – opis techniczny i instrukcja eksploatacji*. Warszawa: Wydawnictwo MON.

Określenie reakcji dynamicznych występujących w łożyskach rotora zaprojektowanej głowicy skanująco-śledzącej

Daniel GAPIŃSKI

Politechnika Świętokrzyska, Wydział Mechatroniki i Budowy Maszyn,
Al. 1000-lecia PP 7, 25-314 Kielce

Streszczenie. W pracy przedstawiono badania mające na celu określenie reakcji dynamicznych występujących w łożyskach zamontowanych na osi obrotu rotora zaprojektowanej głowicy skanująco-śledzącej. Powyższa głowica przeznaczona jest do wykrywania oraz śledzenia celów powietrznych emitujących promieniowanie elektromagnetyczne w zakresie podczerwieni. W badaniach uwzględnione zostały reakcje dynamiczne pochodzące od ruchu obrotowego rotora, jak również reakcje wynikające z przeciążeń działających na głowicę w trakcie lotu pocisku rakietowego. Wyniki badań zaprezentowano w formie graficznej.
Słowa kluczowe: reakcje dynamiczne, mechatronika, głowica samonaprowadzająca, wykrywanie i śledzenie celów